Manzala lagoon, Nile delta, Egypt: modern sediment accumulation based on radioactive tracers

L. K. Benninger · I. B. Suayah · D. J. Stanley

Abstract This study was undertaken to determine whether recent anthropogenic changes in the Nile basin have affected the modern rate of sediment accumulation in the Nile delta. Excess ^{210}Pb, ^{137}Cs, and ^{239,240}Pu were used to develop a sediment chronology for a core from central Manzala lagoon, the delta sector which has had the highest average rate of sediment accumulation during the Holocene (to about 0.7 cm year^{-1}). Excess ^{210}Pb was detected in the top 32 cm of the core, yielding an accumulation rate of 1.2 cm year^{-1}, higher than the mean rate for the Holocene. A high ^{137}Cs/^{239,240}Pu ratio requires a reactor source (possibly Chernobyl) for these nuclides. Low concentrations of excess ^{210}Pb and weapons-fallout nuclides precluded recognition of changes in sediment accumulation rate in Manzala lagoon during this century and may limit the use of tracer radionuclides for modern sediment chronology in the Nile delta.

Key words Manzala lagoon · Nile delta · Chernobyl · Radionuclides

Introduction

Manzala lagoon, the largest wetland in Egypt's Nile delta, has been considerably altered by human activity since its formation more than 3000 years ago. However, more change has occurred during the past two centuries than during the lagoon's entire previous history (Jacotin 1818; Stanley and Warne 1993). The rate of modern sediment accumulation, based upon particle-reactive radionuclide

L. K. Benninger (✉) · I. B. Suayah
Department of Geology, CB #3315 Mitchell Hall, University of North Carolina, Chapel Hill, NC 27599-3315, USA
Tel.: +1 919 962-0699 · Fax: +1 919 966 4519

D. J. Stanley
Deltas-Global Change Program, Paleobiology E-206, National Museum of Natural History, Smithsonian Institution, Washington, DC 20560, USA
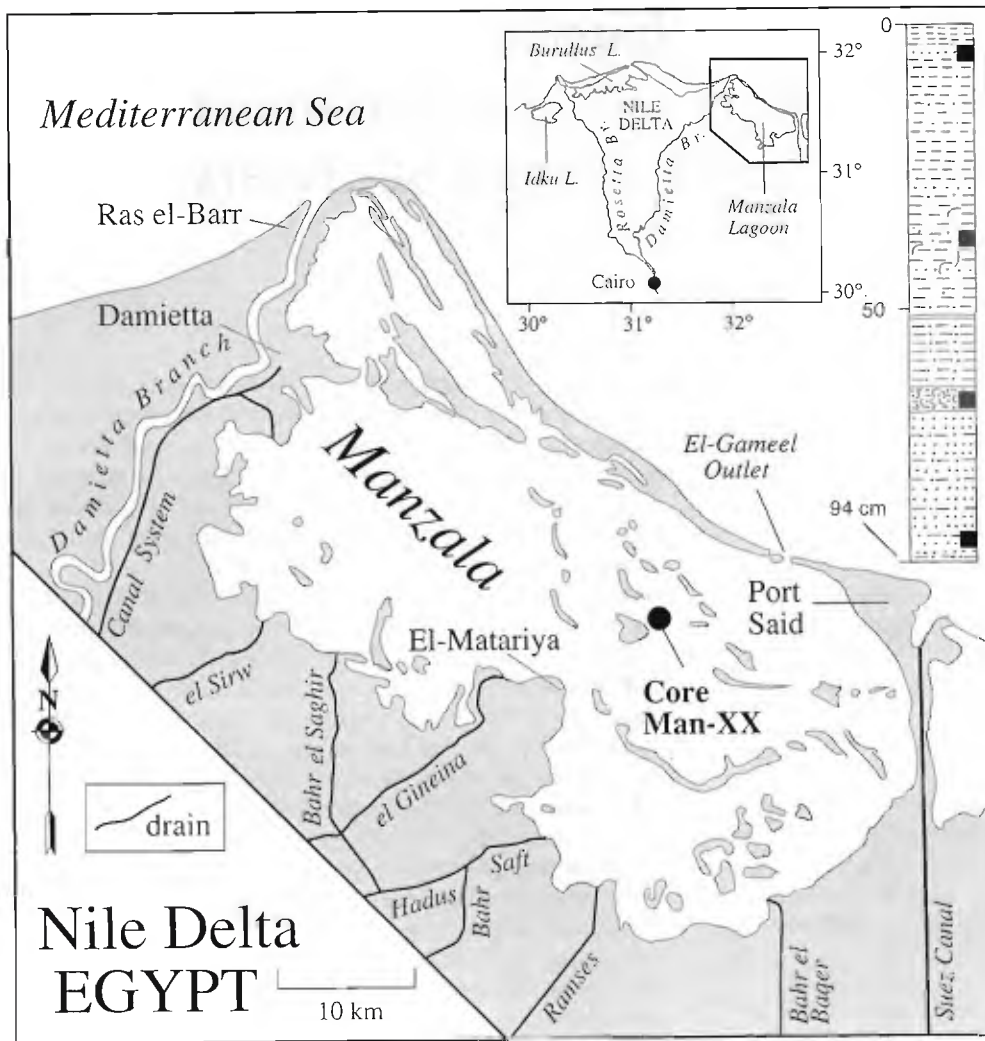
tracers in a short sediment core from Manzala lagoon, was estimated so as more accurately to document recent changes in this important wetland. Two byproducts of the sediment chronology were: (1) evidence for reactor-derived (possibly Chernobyl) radionuclides in Manzala lagoon; and (2) an illustration of the challenge of modern sediment chronology in arid northern Africa.

Maximum dimensions of the rectangular lagoon (Fig. 1) are 49 km (NW-SE) by 29 km (SW-NE). Annual water temperature ranges from 14 to 34 °C, and salinity from 0.68 g l^{-1} in winter to >3.0 g l^{-1} in summer. Until emplacement of the Aswan High Dam, the amount of freshwater flowing into the lagoon ranged from about 300×10^6 m^3 in winter, to about 550×10^6 m^3 in early fall (El-Hehyawi 1977). The suspended load varied seasonally from 0.22 to 0.40 g l^{-1}, with an annual input of ~450 000 tons (El-Wakeel and Wahby 1970b). A useful compilation of references pertaining to Manzala lagoon is available in Kerambrun (1986).

Along most of its northern margin, Manzala is separated from the Mediterranean Sea by a series of broad, elongate, coalescing, low-elevation sand ridges. The Suez Canal, when completed in 1869, formed Manzala's eastern boundary. Since the mid-19th century, the volume of water flowing seaward in the Damietta branch of the Nile, which forms the lagoon's western border, has decreased markedly. This is a function of artificially increased channelization of this Nile branch and diversion of Nile water into an increasingly complex agricultural canal system (Stanley 1996). By 1902, emplacement of several barrages across the River Nile and construction of the lower dam at Aswan in Upper Egypt resulted in a more even annual freshwater flow into the lagoon and reduction of the late-summer early-fall Nile flood effects (Hurst 1944; Waterbury 1979).

Most significant in minimizing effects of the annual Nile flood and in controlling the volume of Nile water flowing northward to Cairo and the Nile delta was closure of the High Dam at Aswan in 1964. Since the dam's construction, the volume of water and sediment bypassing the delta coast through the Nile distributaries has diminished markedly, and flood waters no longer breach the Nile's channelized Damietta branch. Thus, Manzala lagoon no longer so directly records a seasonally important flood sediment input. Most changes in the lagoon's hydrology and sediment processes during the past three decades have resulted from increasingly controlled and diverted

Fig. 1
Map showing position of core Man-XX collected in Manzala lagoon, in the northeastern Nile delta of Egypt (see inset). Four *black squares* in the core log denote positions of samples (approximately 4, 36, 64, 88 cm) analyzed for grain size and composition of the sand size fraction (in text)

water flow across the delta by an increasing number of canals of varying size and drains. These carry ever larger amounts of waste water, solids, and suspensates from the southern and northeastern delta into the southern sector of the lagoon (Fig. 1). Moreover, land reclamation projects and conversion of marshes to aquacultural ponds and farmland along the western, southern, and eastern Manzala margins, have decreased the lagoon area from >200 000 to <160 000 ha.

Since completion of the High Dam 32 years ago, the population in the Nile delta, including Cairo, has increased to >40 million. During this period, the region has experienced increased industrialization as well as altered agricultural practices, and as a consequence, the amount of municipal, agricultural and industrial wastes, and associated pollutants discharged into Manzala via the waterways is rising (Siegel and others 1994, 1995). This increased proportion of effluent and sediment is now pumped directly into southern and western lagoon sectors via the large number of canals and drains, and a series of small mud-rich deltas have formed at waterway mouths. Excess water carrying suspended sediment is discharged from Manzala lagoon through El-Gameel outlet

10 km west of Port Said (Stanley 1996). However, until now it could only be surmised that this lagoon of decreasing size has continued to serve as an important sediment trap during the past three decades. No rates of sediment accretion have been directly determined. The last systematic analysis of modern Manzala sediments dates back to the late 1960s (El-Wakeel and Wahby 1970a), shortly after closure of the High Dam. In that study, 46 surficial samples collected in most lagoon sectors were examined for grain size, moisture, and chemistry (including organic matter, carbon, nitrogen, phosphorus, and iron content). More recent studies of continuous Holocene sediment sections in drill cores collected in this region have recorded changes through time in environments, long-term sedimentation rates, and compositional variations in sand and clay size fractions (Coutellier and Stanley 1987; Stanley 1988; Siegel and others 1995).

A new study has been initiated on 83 surficial samples and 30 short cores collected throughout the lagoon in 1990 (G. Randazzo and D. J. Stanley, in preparation) in order to define the most recent evolution of the uppermost sediment column. The present investigation focuses specifically on the recent rate of sediment accumulation

in the central lagoon, a sector distal from mouths of canals and drains, marshes, and the major lagoon outlet.

Modern sediment chronology with radioactive tracers

The modern sediment chronology which is reported here for core Man-XX is based upon the distribution of particle-reactive radionuclide tracers in the sediment column. A chemical species is described as 'particle-reactive' if it displays a high affinity for the solid phase, and, correspondingly, a low solubility. Particle-reactive chronometric tracers are assumed to associate irreversibly with sediment particles and thus to trace vertical transport of those particles in the sediment column by mixing or sediment accumulation.

Natural excess ^{210}Pb and artificial radionuclides (^{137}Cs, ^{239,240}Pu) were used as chronometric tracers. ^{210}Pb (half-life 22.26 years) is a daughter in the ^{238}U decay series, and *excess* activity is calculated as the difference between total ^{210}Pb and ^{226}Ra (half-life 1600 years), the nearest long-lived progenitor radionuclide. The necessity of precisely determining the difference in activities between ^{210}Pb and ^{226}Ra limits chronology with excess ^{210}Pb, in the most favorable cases, to about five half-lives, or 110 years. In most shallow-water environments excess ^{210}Pb derives largely from the deposition of ^{210}Pb from the atmosphere, where it is produced by decay of gaseous ^{222}Rn. Following rapid adsorption from the water column, ^{210}Pb is delivered to the sediment-water interface by sediment deposition and transported within the sediments by accumulation and mixing. In interpreting sediment profiles of excess ^{210}Pb one usually assumes at least a steady-state in input of ^{210}Pb, and frequently also steady-state rates of sediment accumulation and sediment mixing. ^{137}Cs and the Pu isotopes occur in the environment as byproducts of processes which exploit nuclear fission. Dispersal has resulted from atmospheric weapons testing, leakage from nuclear reactors, and reprocessing of reactor fuel. Releases from reactors and reactor fuel are generally significant locally or regionally, depending upon the magnitude of the release. For example, the Chernobyl accident of April–May 1986 released large quantities of fission-product radionuclides, including ^{137}Cs (Khan 1990); however, while Chernobyl radionuclides were detected worldwide, deposition of Chernobyl activity was concentrated over Europe (for example, Gudiksen and others 1989). In contrast, atmospheric fallout from weapons testing was global in distribution, though concentrated in the northern hemisphere (Joseph and others 1971). Sediment chronology using artificial radionuclides depends upon a known history of radionuclide input. Accidental releases (for example, Chernobyl) have occurred during short, well-known intervals of time. Most weapons-fallout occurred between the mid-1950s and the late 1960s, with two time-points potentially recognizable in sediments: earliest input, about 1953, and maximum atmospheric deposition in 1963. Inputs of artificial radionuclides from reactor releases or fuel reprocessing generally differ from global fallout in isotopic composition, as well as in history. In summary, combining excess ^{210}Pb and artificial radionuclides in chronologic studies provides independent tracers with overlapping time-scales, a significant advantage in interpretation of results.

Methods

Sampling and general petrology

In September 1990, core Man-XX (94 cm in length, 12 cm diameter) was collected in Manzala lagoon at a depth of 1.20 m about 9 km northeast of the town of El-Mataria, 1 km northeast of Lagân island and 10 km southwest of El-Gameel outlet (Fig. 1). This sampling site is close to that of surficial sample #11 collected in the late 1960s by El-Wakeel and Wahby (1970a). The core was examined using X-radiography (Fig. 2), grain size was measured by means of a laser coulter counter, and composition was determined for the sand-size fraction (cf. Coutellier and Stanley 1987).

Chemistry and radiochemistry

Manzala samples of dry masses 20–40 g were first gamma-counted on an intrinsic Ge detector, as described in Benninger and Wells (1993). Samples were sealed tightly to prevent escape of ^{222}Rn and stored prior to counting for at least 2 weeks to ensure secular equilibrium between ^{222}Rn and ^{226}Ra. Most samples were counted during July–October 1991, but a second group of samples (8–10, 12–15, 17–20, and 22–25 cm) was obtained in August 1996 and counted in September 1996. Gamma spectra were analyzed to yield activities of: ^{137}Cs (photopeak at 662 keV); ^{226}Ra (via photopeaks of ^{214}Pb at 295 and 352 keV and ^{214}Bi at 609 keV); ^{228}Ra (via ^{228}Ac photopeaks at 911 and 969 keV, plus, for depths below ca 10 cm, the ^{212}Pb and ^{208}Tl photopeaks at 239 and 583 keV, respectively); ^{40}K (photopeak at 1461 keV). In addition, spectra were examined for the presence of the 604.7-keV photopeak due to ^{134}Cs, but this nuclide was not quantified. ^{137}Cs activities were decay-corrected (half-life 30.0 years) to the date of core collection (15 September 1990). For K only, the results of gamma spectrometry are reported in (μmol K)g^{-1}, assuming the same isotopic composition of K in samples and standards.

Because the Manzala sediments were visibly heterogeneous mixtures of coarse carbonate shell fragments and terrigenous sand and mud, subsamples for wet-chemical analyses were prepared by passing the bulk sediment through a riffle-type splitter. Carbonate-C was determined on about 5 g of sediment by weighing on Ascarite ($^{®}$) the CO_2 evolved with dilute HCl; the technique was essentially that of Hillebrand and others (1953), modified to replace the absorption tubes with low-pressure chromatographic columns.

^{210}Pb (via its granddaughter ^{210}Po) and ^{239,240}Pu were determined separately in the solution and the solid residue resulting from the carbonate analysis. The solution was

Fig. 2
X-radiographic print showing laminations (L) near top of core Man-XX, and molluscan (mostly *Cardium*) debris including some closed bivalves, mixed in sandy and silty mud

separated by settling and decantation, and the residue was collected by drying. After filtration the solution received isotopic tracers (^{209}Po and ^{242}Pu), and the radionuclides were scavenged by precipitation of Fe and Mn hydroxides. The dried residue was transferred to a microwave digestion bomb, spiked with the same isotopic tracers, and totally dissolved by microwave heating of a HF-HNO$_3$ acid mixture.
To eliminate HF and excess HNO$_3$ the digestion mixture was evaporated with 2 ml H$_2$SO$_4$. Then the solid residue

was redissolved in dilute HNO$_3$ and the radionuclides scavenged by precipitating Fe and Mn, as in the foregoing. Po isotopes were separated by spontaneous deposition onto Ag disks from 1 M HCl and determined by alpha spectrometry. Excess ^{210}Pb was calculated as the difference between total ^{210}Po and ^{226}Ra, decay corrected to 15 September 1990; the effect of ^{222}Rn loss from the sediment on excess ^{210}Pb (Imboden and Stiller 1982) was neglected. Pu isotopes were separated by anion-exchange chromatography (Anderson and Fleer 1982), then electrodeposited on stainless steel disks (Benninger and Dodge 1986) for alpha spectrometry.

Results

Core description
Olive-gray clayey silt and sand forms the top 64 cm of core Man-XX, and distinct laminations are noted in the upper 10 cm of the core (Fig. 2). Below 10 cm bioturbated zones include molluscs in sandy silt layers. A grayish, 2-cm-thick shell concentrate (hash layer), formed primarily of molluscan debris (mostly *Cardium*), occurs at 64–66 cm. Below this coquina lies a 28-cm-thick sequence of indistinctly stratified, dark-olive-gray mix of clayey silt and fine sand. Grain-size analyses of four samples (positions at 4, 36, 64, and 88 cm denoted on core log in Fig. 1) record the following range of values: >2 mm fraction, comprising mostly molluscan shell and debris, 7–17%; sand fraction, 30–41%; silt fraction, 31–58%; and clay fraction, 8–38%. The sand fraction comprises 3–12% heavy minerals, 1–4% mica, 4–20% benthic foraminifera, 1–38% ostracods, 4–15% molluscan shell debris, and about 1% plant matter. At the time the core was recovered, a surficial sample (Man-52) was also taken at the same locality. This sample comprises a mix of sand, silt, and clay; the sand fraction includes about 1% heavy minerals, 4% mica, 12% foraminifera, 11% ostracods, 44% molluscan debris, and 7% plant matter. Most important volumetrically is molluscan debris, which accounts for over two-fifths of the sand-size fraction.

Carbonate content and gamma spectrometry
The core description, X-radiograph (Fig. 2), and visual inspection of subsamples all revealed that core Man-XX contained abundant shells and shell fragments over some depth intervals. Figure 3 displays results of the carbonate-C analyses, as (mmol C)g^{-1}; multiplying these values by 10 gives a close approximation to the equivalent mass percentages as CaCO$_3$. Two duplicate analyses are shown, at 2–4 cm and 30–32 cm; the substantial difference (0.4 mmol g^{-1}) in the latter interval is probably a real difference between two sample splits. Overall, the data in Fig. 3 portray a simple pattern of variability: high (≥ 3 mmol g^{-1}) carbonate-C in the top 50 cm, decreasing below 50 cm to low values (<1 mmol g^{-1}) at depths >70 cm. The lowest value, ~0.04 mmol g^{-1} at 86–88 cm, is close to the limit of detection in 5-g samples.
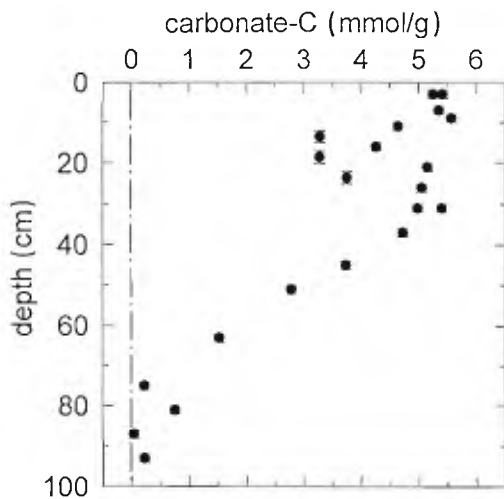
Fig. 3
Carbonate-C, mmol g^{-1} (dry mass basis), in Manzala core Man-XX. Multiplying abscissa values by 10 gives the approximate equivalent in mass percent CaCO$_3$ (assumed pure)

Fig. 4
K and ^{228}Ra (reflecting ^{232}Th) are associated mainly with detrital phases and are therefore diluted by carbonate in Manzala core Man-XX. When expressed on a carbonate-free basis, concentrations of K and Th are nearly constant, implying uniform composition of the detrital fraction of the sediment. *Horizontal dashed lines* show average concentrations, 2–94 cm for K, 10–94 cm for ^{228}Ra. *Vertical error bars* are one-sigma uncertainties, propagated from counting statistics.
t Bq = t disintegration s^{-1}

As a chemical test for uniformity of lithology, Fig. 4 shows depth profiles of K and ^{228}Ra (representing ^{232}Th), both recalculated on a carbonate-free basis. This calculation assumes that the carbonate-C (Fig. 3) existed in the sediment as pure CaCO$_3$. Coefficients of variation for carbonate-free K and ^{228}Ra were 11.7% and 10.3%, respectively, suggesting that the detrital fraction of the sediment did not vary extensively in composition.
^{226}Ra (Fig. 5) varied significantly at depths < 60 cm, whether expressed on a total-mass or a carbonate-free basis; convergence of the total-mass and carbonate-free concentrations below 60 cm resulted from low carbonate deep in the core (Fig. 3). Unlike ^{228}Ra, which as a short-lived nuclide (half-life 5.75 years) largely tracks parent ^{232}Th, ^{226}Ra is sufficiently long-lived (half-life 1600 years) to exhibit significant mobility to tens of centimeters into the sediment column.

Chronometric tracers

The depth profile of excess ^{210}Pb in Manzala core Man-XX is shown in Fig. 6a. Activities of excess ^{210}Pb were clearly low, with the maximum < 10 Bq kg^{-1}. By way of comparison, surficial activities of excess ^{210}Pb in seven cores from the Neuse River estuary, North Carolina, varied between 140 and 210 Bq kg^{-1} (Benninger and Wells 1993). Combined with the large uncertainties in ^{226}Ra (Fig. 5), low activities of total ^{210}Pb (excess + supported) yielded very large uncertainties in excess ^{210}Pb. Adopting the convention that excess ^{210}Pb is finite only when it exceeds zero by two standard deviations, the deepest occurrence of excess ^{210}Pb was in the interval 30–32 cm, and four samples within the top 32 cm did not contain finite excess ^{210}Pb (8–10, 10–12, 17–20, and 22–25 cm). The curves plotted in Fig. 6 represent simple models for sediment chronology; these models are discussed in the following.
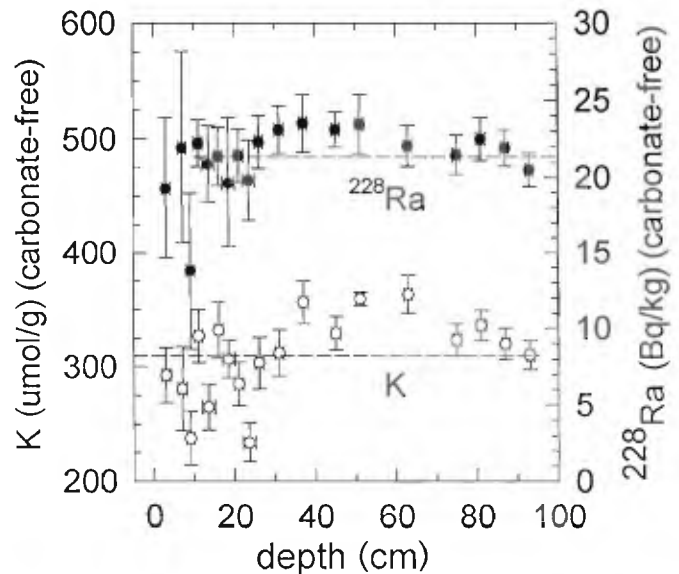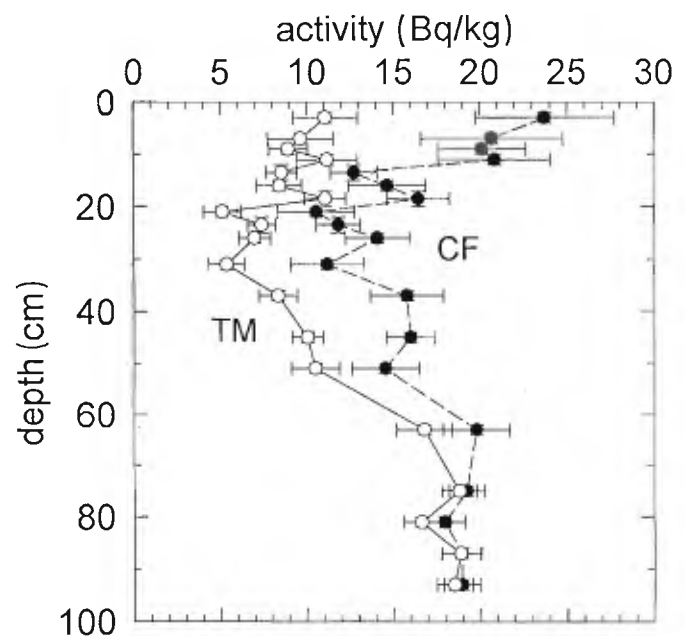

Fig. 5
^{226}Ra is constant only below about 60 cm depth in core Man-XX, whether concentration is expressed on a total-mass basis (TM) or a carbonate-free basis (CF). The long half-life of ^{226}Ra permits significant chemical mobility in the upper tens of centimeters of the core. *Horizontal error bars* are one-sigma uncertainties, propagated from counting statistics.
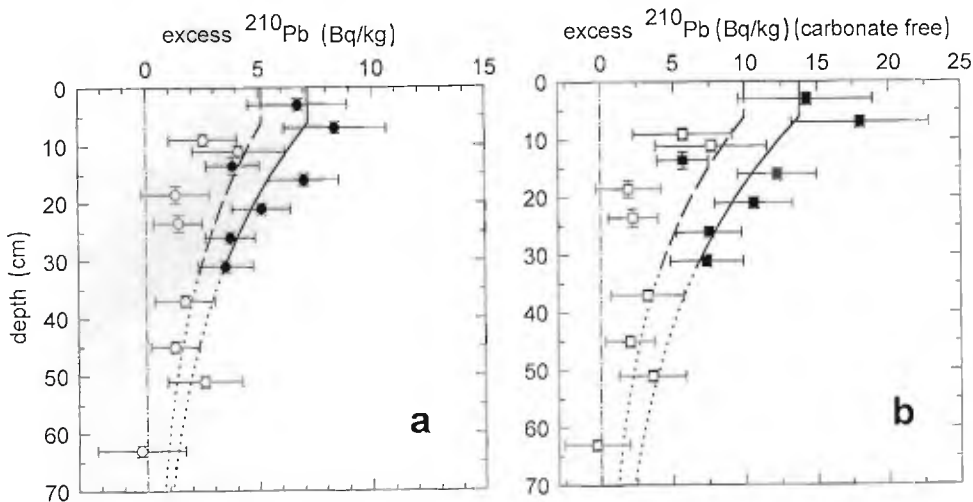t Bq = t disintegration s^{-1}

Fig. 6a, b

Excess ^{210}Pb (a dry-mass basis; b carbonate-free basis) *versus* depth, core Man-XX. *Solid symbols* represent samples in which excess ^{210}Pb was demonstrably finite (exceeded zero by >2 standard deviations). *Horizontal error bars* are 1-sigma uncertainties propagated from counting statistics. Low total ^{210}Pb and large uncertainties in ^{226}Ra produced large errors in excess ^{210}Pb. The *solid curves* from 2–32 cm are the best-fit exponentials to finite values of excess ^{210}Pb; the *dashed curves* fit all data from 2–32 cm; *dotted curves* (32–70 cm) extend the *solid* and *dashed curves* through the deeper samples.
1 Bq = 1 disintegration s^{-1}

Data for the fission-related radionuclides, ^{137}Cs and $^{239,240}Pu$, are presented in Table 1 and Fig. 7. Plutonium is reported as $^{239,240}Pu$ because ^{239}Pu and ^{240}Pu are not resolved by alpha spectrometry. Clearly, finite levels of both tracers were limited to shallow levels in the core. Again defining as finite only those concentrations which exceeded zero by at least two standard deviations, the deepest occurrence of finite ^{137}Cs was in the interval 12–15 cm, while $^{239,240}Pu$ was marginally finite at greater depths in some samples (15–17, 20–22, and 22–25 cm). Table 1 and Fig. 7 include data only to the maximum depth to which at least one of ^{137}Cs or $^{239,240}Pu$ was fin-

ite; additional depth intervals in which these nuclides were sought, but not detected, included all depths >25 cm for ^{137}Cs, but only 25–27 cm, 30–32 cm, and 36–38 cm for $^{239,240}Pu$. Although the profiles in Fig. 7 lack definition in the top 10 cm, it is clear that this interval contained the maximum concentrations of both ^{137}Cs and $^{239,240}Pu$.

Two shallow samples (2–4 cm, 6–8 cm) which were gamma-counted in 1991 contained marginally finite ^{134}Cs. This was detected as low peaks above baseline at 604.7 keV; for 1-day counting times, observed net counts (above baseline) were 115 ± 32 at 2–4 cm and 63 ± 29 at 6–8 cm. For the same counting periods, net counts for ^{137}Cs were 785 ± 39 (2–4 cm) and 787 ± 61 (6–8 cm).

Discussion

Rates of sediment accumulation based on long cores in region

It is of note that short core Man-XX was collected (1) in a sector distal from lagoon margins, marshes, canal and drain mouths and El-Gameel outlet, and (2) in the north-eastern Nile-delta area capping the thickest sequence of
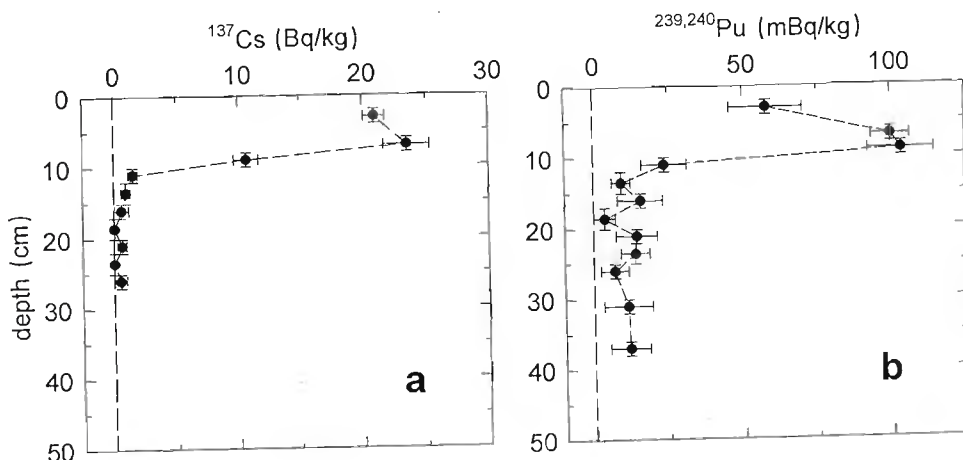

Fig. 7a, b
Artificial radionuclides a ^{137}Cs and b $^{239,240}Pu$ (dry-mass basis) in Manzala core Man-XX. *Horizontal error bars* are 1-sigma uncertainties propagated from counting statistics. Finite levels (exceeded zero by >2 standard deviations) were limited to 15 cm depth for ^{137}Cs, 25 cm for $^{239,240}Pu$. 1 Bq = 1 disintegration s^{-1}

Table 1
^{137}Cs and ^{239,240}Pu in core Man-XX (ND: not detected. Uncertainties are $\pm 1\sigma$, propagated from counting statistics.)

interval, cm	^{137}Cs Bq kg^{-1}	^{239,240}Pu mBq kg^{-1}	^{137}Cs/^{239,240}Pu activity ratio
2–4	21.36 ± 0.85	57.8 ± 12.3	370 ± 80
6–8	24.06 ± 1.88	100.0 ± 6.5	241 ± 24
8–10	12.18 ± 1.15	103.5 ± 11.2	118 ± 17
10–12	1.50 ± 0.39	23.6 ± 7.6	64 ± 26
12–15	1.03 ± 0.42	9.1 ± 3.0	113 ± 60
15–17	ND	15.6 ± 7.5	
17–20	ND	3.6 ± 3.6	
20–22	ND	14.2 ± 6.9	
22–25	ND	13.8 ± 4.9	

Holocene deposits. This eastern lagoon region close to Port Said is underlain by a Holocene section reaching ~ 50 m in thickness (Stanley 1988). This observation is based on at least 20 long drill cores (to 55 m in length), from Smithsonian expeditions and borehole logs from available engineering foundation borings on the periphery and within Manzala lagoon. Most of these cores completely penetrated the dark-olive-gray, mud-rich Holocene and basal grey shelly sand section, and reached the yellowish, oxidized, sandy upper part of the latest Pleistocene unit (Stanley and Warne 1993). Conventional radiocarbon dates determined for the base of dark Holocene deltaic mud sequences in this area range from 7800 to 6500 years B.P. (uncorrected). Long cores have recovered prodelta, delta-front, lagoon, and strandplain facies. Assigning an age of 7500 years to the base of thickest Holocene sections, the minimal mean long-term sediment accumulation rate is about 0.7 cm.year^{-1}; the actual rate is higher if allowance is made for compaction and loss of section by erosion (Goodfriend and Stanley 1996). This high average Holocene rate is consistent with deposition of large amounts of sediment transported by former branches of the Nile (Mendesian, Tanitic, Pelusiac) that previously flowed to this NE delta region (Toussoun 1922; Coutellier and Stanley 1987).

Setting of modern sediment accumulation in Manzala lagoon

Increased effects of eutrophication are recorded in many sectors of Manzala lagoon. Laminated sediments at site Man-XX, however, record periods of active sediment transport and oxidation at the sediment-water interface on this part of the lagoon floor. This activity is largely a function of wind-mixing, primarily in winter. The site, while distant from lagoon margins, wetland mouths and the lagoon outlet, is shallow, and both active sediment transport and deposition occur throughout most of the year. This periodically high-energy sedimentary regime is recorded by petrologic attributes of the core: lamination; a mix of roughly equivalent amounts of sand, silt, and clay; and in the sand fraction, relatively high proportions of mica, heavy minerals and microfossils, and a low plant fragment content. Relatively high proportions of molluscs (assemblages identified by Bernasconi and Stanley 1994) and microfossils (by El-Wakeel and others 1970; Pugliese and Stanley 1991) show that site Man-XX is influenced by freshwater fed at the southern margin of the lagoon, which mixes with seawater entering from the north via El-Gameel outlet and, in winter, via storm waves that overtop the low sand barrier.

It is also noted that site Man-XX, in the east-central part of the lagoon, is positioned above a structurally active basin. This basin, subject to high mean rates of subsidence (to 5 mm year^{-1}) during the Holocene (Stanley 1988, 1990), has continued to accumulate important thicknesses (to 50 m) of sediment until the present. Increased levels of potentially toxic metals, including Hg, Pb, Sn, Zn, Cu, and Ag, are recorded in the upper 20 cm of sediment cores in the southeastern sector of the lagoon (Siegel and others 1994). This demonstrates that sediment is still being delivered to the lagoon (mostly via the dense irrigation channel network) and distributed within the basin by bottom current processes. The volumes of water, sediment, and effluent discharging into the lagoon today are, in fact, accumulating in a nearly enclosed depositional trap of decreasing area. Thus, one could expect high, and still increasing, sediment accumulation rates.

Evidence of reactor-derived radionuclides in core Man-XX

The ^{137}Cs/^{239,240}Pu activity ratios in the samples from the top 15 cm of core Man-XX ranged from 370 ± 80 (2–4 cm) to 64 ± 26 (10–12 cm) (Table 1). Although the ratios are imprecise below 10 cm, all are higher than would be expected from global weapons fallout. "Fresh" fallout debris had an activity ratio of about 84 (Joseph and others 1971; Sholkovitz 1983). Radioactive decay since the main pulse of global fallout during the 1960s would reduce this ratio in a closed system, since the half-life of ^{137}Cs (30 years) is very short compared to the half-lives of the Pu isotopes (^{239}Pu: 24110 years; ^{240}Pu: 6563 years). Geochemistry would further reduce the ^{137}Cs/^{239,240}Pu ratio in sediments deposited from brackish or saline water, since in these circumstances ^{137}Cs must compete with abundant stable alkali metals for sorption sites. The impact of salinity on ^{137}Cs sorption is illustrated in samples from the Neuse River estuary of North Carolina, a coastal sedimentary environment for which global fallout has been the only significant source of ^{137}Cs and ^{239,240}Pu. In seven sediment cores collected in this estuary between 1982 and 1990, the ^{137}Cs/^{239,240}Pu activity ratios at the depth horizons of maximum activities varied between 6 and 30 (Benninger, unpublished data). Radionuclide releases from nuclear reactors have higher ^{137}Cs/Pu activity ratios than global fallout, and input of such material could help to explain the high activity ratios observed in the uppermost samples of core Man-XX. For example, the 1986 accident at Chernobyl in the Ukraine released material with a ^{137}Cs/^{239,240}Pu activity ratio estimated at 600–1200 (Khan 1990). Ratios this high would not be expected in

sediments deposited from water, due to solubility of some fraction of the ^{137}Cs (for example, Erlenkeuser and Balzer 1988).

When recently released from a reactor, ^{137}Cs should be accompanied by ^{134}Cs (half-life 2.06 years) (for example, Joseph and others 1971; Olsen and others 1981), whereas this short-lived Cs isotope has disappeared from global fallout by radioactive decay. Chernobyl fallout had a ^{134}Cs/^{137}Cs activity ratio of about 0.5 (Dörr and Münnich 1987; Khan 1990). During the interval (5.3 years) between the Chernobyl accident and our earliest analyses of shallow samples, this ratio decreased to <0.1. Thus, in small samples, the ^{134}Cs/^{137}Cs activity ratio neither confirmed nor excluded Chernobyl as a source for the radiocesium in core Man-XX. The marginal count rates reported above for ^{134}Cs in samples from 2–4 cm and 6–8 cm were approximately appropriate for Chernobyl fallout, but this is not considered here a definitive result.

Modern sediment chronology

The principles underlying sediment chronology with excess ^{210}Pb have been presented by Robbins (1978). Given the nature of the data from core Man-XX (Fig. 6a) only a very simple approach was justified. Constant fluxes of sediment and of excess ^{210}Pb to the sediment-water interface were assumed. Porosity variations (unknown) were neglected. Decreases in excess ^{210}Pb with depth were fitted with exponential curves. Then three factors determined the models of Fig. 6.

Mixing. It was assumed in all cases that the top 6 cm of core Man-XX was subject to mixing rapid enough to homogenize excess ^{210}Pb over this interval. Strictly speaking, the data did not require a mixed layer: given the noise in excess ^{210}Pb, surficial mixing makes little difference to the models, and laminations and abundant shells near the core top suggest that bioturbation was not intense. However, it is probable that sediment from our core site (Fig. 1), at 1.2 m water depth and in an exposed location, was occasionally resuspended by wind-driven waves. A mixed-layer thickness of 6 cm was chosen because deeper rapid mixing would be incompatible with the distribution of ^{239,240}Pu (Fig. 7b), while data were insufficient to define a mixed layer of lesser thickness.

Finite levels of excess ^{210}Pb. Only samples from the top 32 cm of core Man-XX contained finite excess ^{210}Pb. Accordingly, exponential fits to decreasing excess ^{210}Pb, shown as solid and dashed curves in Fig. 6, were based only upon data from the 0–32 cm depth interval. Within the top 32 cm, two fits to the data are presented in each of a and b of Fig. 6. The solid curve is fitted only to the finite excess ^{210}Pb (exceeds zero by two standard deviations); the dashed fit includes all data within 0–32 cm. To ensure continuous profiles of excess ^{210}Pb, the curve-fit excess ^{210}Pb at 6 cm defines, in all cases, the constant level of excess ^{210}Pb in the interval 0–6 cm. All fits have been extrapolated below 32 cm (dotted curves in Fig. 6) for illustration only.

Total-mass and carbonate-free bases. Core Man-XX contained abundant, but variable, CaCO$_3$ in the top 32 cm.

As shell material probably did not contain significant excess ^{210}Pb, the carbonate might have altered the shape of the profile of excess ^{210}Pb by variably diluting it. Figure 6b illustrates a test for this effect: excess ^{210}Pb was recalculated on a carbonate-free basis, assuming that the carbonate-C in Fig. 3 was present as pure CaCO$_3$. Accounting for variable carbonate content in this way did not appreciably smooth the depth profile of excess ^{210}Pb.

Each of the four exponential curves in Fig. 6 yielded an estimate of a steady-state sediment accumulation rate in the 0–32-cm interval of core Man-XX. With the simple assumptions already described (steady-state inputs of excess ^{210}Pb and of sediment, constant porosity, no sediment-mixing below 6 cm), the distribution of excess ^{210}Pb over the interval 6–32 cm is described by

$$A_Z = A_6 \exp[-(\lambda/s)z],$$

where A_Z = activity of excess ^{210}Pb at depth $z \ge 6$ cm,
A_6 = activity of excess ^{210}Pb at depth 6 cm,
λ = decay constant of ^{210}Pb ($=0.0311$ year^{-1}),
s = rate of sediment accumulation, cm year^{-1},
z = depth in sediment, cm.

Thus rates of sediment accumulation were calculated from the magnitude of the exponential-fit parameter (λ/s), determined by least-squares fitting of $\ln(A_z)$ vs z. The rates so calculated were all similar: the range was 1.0–1.3 cm year^{-1}, the average 1.2 cm year^{-1}. It appears, therefore, to make little difference whether all data are used, or only those which are demonstrably finite, or whether excess ^{210}Pb is expressed on a total-mass or a carbonate-free basis. The data did not justify extending the models below 32 cm. However, it is clear from Fig. 6 that the deeper observations (to 60 cm) are also compatible, within uncertainties, with a sediment accumulation rate of about 1.2 cm year^{-1}.

The ^{210}Pb accumulation rate can be tested against the distributions of the fission-associated nuclides ^{137}Cs and ^{239,240}Pu. The highest concentrations of these nuclides were restricted to the top 10 cm of core Man-XX (Table 1, Fig. 7). Assuming rapid mixing of the top 6 cm and accumulation at 1.2 cm year^{-1}, the fission-associated nuclides would have penetrated to 10 cm during the 3.3 years preceding core collection in September 1990. Thus, since the Chernobyl accident occurred during April–May 1986, the ^{210}Pb sediment chronology is consistent with Chernobyl as the source of the ^{137}Cs and ^{239,240}Pu in the top 10 cm of core Man-XX. Clearly this inference is sensitive to the actual thickness of the surficial, rapidly mixed layer in the core. No other report of Chernobyl fallout over northern Egypt has been found, but several lines of evidence show deposition of Chernobyl nuclides to be plausible. Ammar and others (1987) detected a sharp increase in air-borne radioactivity (650 times normal levels) over Alexandria, Egypt on day 7 of the Chernobyl accident. Gudiksen and others (1989), by modeling the atmospheric dispersion of Chernobyl radionuclides, showed the debris cloud to have reached northern Egypt by day 10 after the initial explosion. Finally, there was no known alternative source of reactor-associated radionuclides.

Within Africa, only South Africa had nuclear reactors as of the end of 1987; Dimona, site of Israeli fuel-reprocessing facilities, though nearby, is in an arid, interior location; European reactors are geographically remote, and French fuel-reprocessing facilities discharge into the North Atlantic (Mounfield 1991).

If all, or most, of the ^{137}Cs and ^{239,210}Pu in the top 10–15 cm of core Man-XX was derived from Chernobyl fallout, then input of these same nuclides to Manzala lagoon from global weapons fallout must have been very low. With a 6-cm mixed layer and sediment accumulation at 1.2 cm year^{-1}, the 1963 maximum in weapons fallout would be expected at about 38 cm depth in the core. The sample from 36–38 cm contained detectable levels of neither ^{137}Cs nor ^{239,240}Pu. Indeed, ^{137}Cs was undetectable in all samples below 15 cm. Thus it appears that global weapons fallout was virtually absent from core Man-XX. This point is further considered below in our discussion of radionuclide inventories.

As already noted, closure of the Aswan High Dam in 1964 controlled water discharge from the Nile and minimized sediment delivery to the delta by the annual flood. A reduced flux of sediment after 1964 might have caused a reduced rate of sediment accumulation in Manzala lagoon. At 1.2 cm year^{-1} about 31 cm sediment would have accumulated between 1964 and 1990 (date of core collection); evidence of a different sediment accumulation rate prior to 1964 would therefore lie at depths >31 cm, where excess ^{210}Pb was not finite. Thus it is not possible to estimate the pre-1964 sediment accumulation rate or to assess the impact of the High Dam closure. Based upon extrapolations below 32 cm of our ^{210}Pb model curves, however, there is no reason to invoke a drastically different rate of sediment accumulation prior to 1964. High rates of sediment accumulation in Nile-delta wetlands are likely to have been maintained after 1964 by an increased efficiency of sediment-trapping in basins of decreasing size. Increased proportions of sediment are introduced through the dense network of irrigation and drain channels in the Nile delta (Stanley 1996).

Closure of the Aswan High Dam might have altered the bulk composition of sediment accumulating in Manzala lagoon, even if the rate of sediment accumulation was not detectably changed. It was already suggested here, on the basis of Fig. 4, that the detrital fraction was of essentially uniform composition in core Man-XX. On the other hand, the top 32 cm of core Man-XX contained, on average, substantially more carbonate than the remainder of the core (Fig. 3). Indeed, the carbonate contents in the top 32 cm (to >50% dry mass as $CaCO_3$) were high enough to contribute significantly to the bulk sediment accumulation rate of 1.2 cm year^{-1}. As noted, carbonate appeared to decrease smoothly below 32 cm in core Man-XX. This overall pattern of variation in carbonate with depth could reflect changing conditions in Manzala lagoon (favoring more production of $CaCO_3$ toward the present), changing sources of sediment to the site of core collection, or progressive dissolution of $CaCO_3$ during early diagenesis. While the highest carbonate concentra-

tions were found in sediments dated as having accumulated post-1964, the variation in carbonate below 32 cm suggests that closure of the Aswan High Dam was not the only factor to affect carbonate concentration in core Man-XX.

Siegel and others (1994) based their estimate of the sediment accumulation rate in Manzala lagoon upon long-term average accumulation rates and a preliminary version of the ^{137}Cs data for core Man-XX (core XX of Siegel and others 1994). The present interpretation of the more complete radionuclide data (^{210}Pb and ^{239,240}Pu, as well as ^{137}Cs) differs from that offered by Siegel and others (1994). Moreover, it is unlikely that modern sediment accumulation rates are constant throughout Manzala lagoon, as implied by Siegel and others (1994). As discussed in the foregoing, core Man-XX was recovered from near the area of maximum Holocene accumulation, but distal from the principal present sediment sources to Manzala lagoon. Higher modern accumulation rates should be expected in sectors close to the mouths of major waterways draining into Manzala lagoon.

Although uncertainties remain, it is of note that the estimated modern rate of sediment accumulation at site Man-XX (~ 1.2 cm year^{-1}) is somewhat higher than the long-term mean Holocene rate (~ 0.7 cm year^{-1}). The implication of this result is that extensive recent changes induced by the High Dam at Aswan have not diminished the sediment accumulation rate in Manzala lagoon.

Inventories of tracer radionuclides in core Man-XX

Total quantities per unit sediment area (that is, sediment "inventories") of excess ^{210}Pb and the fallout radionuclides can convey information about modern sedimentation: sediment sources, processes, and patterns of sedimentation (for example, Benninger and Wells 1993). To obtain the inventories one integrates the activity-depth profiles, taking sediment porosity and solids density into account. In well-studied areas, the sediment inventories can be compared with the inventories expected from direct atmospheric deposition, potentially revealing sites of focusing of modern sedimentation. Where estimates of direct atmospheric deposition are lacking, sediment inventories help to constrain these values.

The inventory of excess ^{210}Pb in Manzala core Man-XX was estimated by integrating the model fits to the excess ^{210}Pb data in Fig. 6a (bulk-sediment, dry-mass data set). For the interval 0–6 cm the concentration of excess ^{210}Pb was taken as defined by the exponential fits over 6–32 cm (dashed and solid curves in Fig. 6a). Constant porosity (0.75) and solids density (2.5 g cm^{-3}) were assumed. Calculations were performed for two different depth limits of integration. If excess ^{210}Pb was finite only to 32 cm depth, the integration from 0 to 32 cm yields an inventory of about 740 Bq m^{-2} (all data, 0–32 cm) or 1110 Bq m^{-2} (finite excess ^{210}Pb only, 0–32 cm). Extending the integration to infinite depth increases these inventories to about 1370 and 1770 Bq m^{-2}, respectively. While the data in Fig. 6 do not precisely establish the inventory, the "true" inventory of excess ^{210}Pb in

core Man-XX is likely to fall within the limits 740–1770 Bq m^{-2}. At steady-state these bounds are equivalent to total ^{210}Pb input fluxes of 23 to 55 Bq m^{-2} year^{-1}, partitioned somehow between direct atmospheric deposition and sediment inputs. There appear to be no published estimates of the atmospheric flux of excess ^{210}Pb elsewhere in the Nile delta. Two estimates are available for northern Israel. Stiller and Imboden (1986) estimated atmospheric deposition of excess ^{210}Pb at 25 Bq m^{-2} year^{-1} at Lake Kinneret. Based upon sediment cores from drained fishponds near Haifa, Krom and others (1994) estimated the atmospheric flux of excess ^{210}Pb at Haifa to be 69 ± 21 Bq m^{-2} year^{-1}. Northern Israel receives considerably higher precipitation than the Nile-delta, and presumably, therefore, a significantly higher atmospheric flux of excess ^{210}Pb. Taking this into account, it is likely that a large share of the inventory of excess ^{210}Pb in core Man-XX was supplied via sediment input to, or sediment focusing within, Manzala lagoon.

Inventories of ^{137}Cs and ^{239,240}Pu in core Man-XX were estimated from data in Table 1. Again invoking a 6-cm mixed layer, it was assumed that the entire 0–6-cm interval contained the same concentrations as reported for the interval 2–4 cm. As for excess ^{210}Pb, constant porosity of 0.75 and constant solids density of 2.5 g cm^{-3} were assumed. The estimated inventories are then ~ 1300 Bq m^{-2} for ^{137}Cs and 5.8 Bq m^{-2} for ^{239,240}Pu. Comparable data for other locations in the Nile delta are lacking. However, two studies provide perspective on the estimated ^{137}Cs inventory in core Man-XX. In the first, Stiller and Assaf (1973) reported total weapons-fallout ^{137}Cs at Nahal Soreq, Israel (ca 31° 54′ N) as 2420 Bq m^{-2}, decay corrected to December 1971; neglecting fallout deposition after 1971 and correcting for decay to September 1990, this value becomes 1570 Bq m^{-2}. Therefore, while the ^{137}Cs in core Man-XX probably derived from a reactor (or reactors), not from atmospheric weapons-testing, it is likely that the sediment inventory of ^{137}Cs equaled or exceeded that which would have resulted from direct atmospheric deposition of weapons fallout over the Nile delta. In the second study, Dörr and Münnich (1987) analyzed soil cores to estimate deposition of Chernobyl ^{137}Cs at 2000 ± 1000 Bq m^{-2} for northern and southwestern Germany. This figure is similar to the ^{137}Cs inventory in core Man-XX, despite the fact that the Chernobyl source should have been much weaker over northeastern Africa (Gudiksen and others 1989). Therefore, as for excess ^{210}Pb, much of the ^{137}Cs inventory in core Man-XX probably resulted from sediment input or focusing. That is, for both excess ^{210}Pb and ^{137}Cs, sediment inventories in core Man-XX substantially overestimate the direct supply of these nuclides to the lagoon surface by atmospheric deposition.

As noted already, the apparent absence of weapons-fallout radionuclides at depths predicted from the ^{210}Pb sediment chronology presents a problem for the chronology in core Man-XX. Thus, it is appropriate to ask what quantities of weapons fallout should be expected in the lower Nile basin. Direct measurements of weapons-fallout deposition over northeastern Africa are very few (HASL 1977). Existing data suggest that two factors could explain the low inventories of weapons-fallout nuclides in core Man-XX. First, the lower Nile (Egypt and Sudan) receives little precipitation, so that little weapons fallout was directly deposited in this region. Second, closure of the Aswan High Dam in 1964 probably largely prevented augmentation of the direct atmospheric deposition by sediment transport from the wetter upper Nile basin. Given these circumstances, the flux of weapons fallout to Manzala lagoon could well have been very weak, perhaps largely obscured by a high sediment flux.

Conclusions

The modern rate of sediment accumulation in the northeastern Nile-delta, as determined by particle reactive chronometric tracers (1.2 cm year^{-1}), is somewhat higher than the mean rate of accumulation during the past 7500 years. At first glance, one could envision that the High Dam, which has so dramatically altered the water flow and sedimentation regime of the lower Nile since 1964, would have induced a dramatically decreased sedimentation rate. However, high modern rates of sediment accumulation are not surprising, given the high inputs of water, sediment, and effluent, flowing via the irrigation and drain channel network into a lagoon whose area is decreasing.

Modern sediment chronology, based upon excess ^{210}Pb and fission-product radionuclides, has been little practiced in north Africa, and to the best of our knowledge there have been no other such studies in the Nile basin. The present results suggest that such chronology in the Nile delta will be challenging, owing to low fluxes of the tracer radionuclides, diluted in high fluxes of sediment. Regional fluxes of both excess ^{210}Pb and weapons-fallout nuclides appear to be low. In Manzala core Man-XX inputs of reactor-derived ^{137}Cs, whether from Chernobyl or from some other source, apparently exceeded inputs of this nuclide from global weapons fallout.

References

Ammar EA, El-Khatib AM, Wahba AG, Elraey M (1987) Radioactive contamination from Chernobyl accident over Alexandria city. Isotopenpraxis 23:303–305

ANDERSON RF, FLEER AP (1982) Determination of natural actinides and plutonium in marine particulate material. Anal Chem 54:1142–1147

BENNINGER LK, DODGE RE (1986) Fallout plutonium and natural radionuclides in annual bands of the coral *Montastrea annularis*, St. Croix, U.S. Virgin Islands. Geochim Cosmochim Acta 50:2785–2797

BENNINGER LK, WELLS JT (1993) Sources of sediment to the Neuse River estuary, North Carolina. Mar Chem 43:137–156

BERNASCONI MP, STANLEY DJ (1994) Molluscan biofacies and their environmental implications, Nile delta lagoons, Egypt. J Coastal Res 10:440–465

COUTELLIER V, STANLEY DJ (1987) Late Quaternary stratigraphy and paleogeography of the eastern Nile delta, Egypt. Mar Geol 77:257–275

DÖRR H AND MÜNNICH KO (1987) Spatial distribution of soil ^{137}Cs and ^{134}Cs in West Germany after Chernobyl. Naturwissenschaften 74:249–251

EL-HEHYAWI MLE (1977) Some aspects of chemistry of lake Manzala water. Bull Inst Oceanogr Fish ARE 7:2–30

EL-WAKEEL SK, WAHBY SD (1970a) Bottom sediments of lake Manzalah, Egypt. J Sediment Petrol 40:480–496

EL-WAKEEL SK, WAHBY SD (1970b) Hydrography and chemistry of lake Manzalah, Egypt. Arch Hydrobiol 67:173–200

EL-WAKEEL SK, ABDOU HF, WAHBY SD (1970) Foraminifera from bottom sediments of lake Maryut and lake Manzalah, Egypt. Bull Inst Oceanogr Fish ARE 1:429–448

ERLENKEUSER H, BALZER W (1988) Rapid appearance of Chernobyl radiocesium in the deep Norwegian Sea sediments. Oceanol Acta 11:101–106

GOODFRIEND GA, STANLEY DJ (1996) Reworking and discontinuities in Holocene sedimentation in the Nile delta: documentation from amino acid racemization and stable isotopes in mollusk shells. Mar Geol 129:271–283

GUDIKSEN PH, HARVEY TF, LANGE R (1989) Chernobyl source term, atmospheric dispersion, and dose estimation. Health Phys 57:697–706

HASL (1977) Final tabulation of monthly 90Sr fallout data: 1954–1976. Health and Safety Laboratory Environmental Quarterly, No. HASL-329. Energy Research and Development Administration, New York

HILLEBRAND WF, LUNDELL GEF, BRIGHT HA, HOFFMAN JI (1953) Applied inorganic analysis. Wiley, New York

HURST HE (1944) A short account of the Nile Basin. Government Press, Cairo

IMBODEN DM, STILLER M (1982) The influence of radon diffusion on the ^{210}Pb distribution in sediments. J Geophys Res 87:557–565

JACOTIN PM (1818) Carte topographique de l'Egypte et de plusieurs parties des pays limitrophes. Paris, 47 plates

JOSEPH AB, GUSTAFSON PF, RUSSELL IR, SCHUERT EA, VOLCHOK HL, TAMPLIN A (1971) Sources of radioactivity and their characteristics. In: Radioactivity in the marine environment. National Academy of Sciences, Washington DC, pp 6–41

KERAMBRUN P (ed) (1986) Coastal lagoons along the southern Mediterranean coast (Algeria, Egypt, Libya, Morocco, Tunisia). Description and bibliography. UNESCO Reports in Marine Science, Paris

KHAN SA (1990) The Chernobyl source term: a critical review. Nucl Saf 31:353–374

KROM MD, KAUFMAN A, HORNUNG H (1994) Industrial mercury in combination with natural ^{210}Pb as time-dependent tracers of sedimentation and mercury removal from Haifa Bay, Israel. Estuarine Coastal Shelf Sci 38:625–642

MOUNFIELD PR (1991) World nuclear power. Routledge, London

OLSEN CR, SIMPSON HJ, TRIER RM (1981) Plutonium, radiocesium and radiocobalt in sediments of the Hudson River estuary. Earth Planet Sci Lett 55:377–392

PUGLIESE N, STANLEY DJ (1991) Ostracoda, depositional environments and late Quaternary evolution of the eastern Nile delta, Egypt. Quaternario 4:275–302

ROBBINS JA (1978) Geochemical and geophysical applications of radioactive lead. In Nraigu JO (ed) The biogeochemistry of lead in the environment. Part A ecological cycles. Elsevier/North Holland, Amsterdam pp 285–393

SHOLKOVITZ ER (1983) The geochemistry of plutonium in fresh and marine water environments. Earth Sci Rev 19:95–161

SIEGEL FR, SLABODA ML, STANLEY DJ (1994) Metal pollution loading, Manzalah Lagoon, Nile Delta, Egypt: implications for aquaculture. Environ Geol 23:89–98

SIEGEL FR, GUPTA N, SHERGILL B, STANLEY DJ, GERBER C (1995) Geochemistry of Holocene sediments from the Nile delta. J Coastal Res 11:415–431

STANLEY DJ (1988) Subsidence in the northeastern Nile delta: rapid rates, possible causes, and consequences. Science 240:497–500

STANLEY DJ (1990) Recent subsidence and northeast tilting of the Nile delta, Egypt. Mar Geol 94:147–154

STANLEY DJ (1996) Nile delta: extreme case of sediment entrapment on a delta plain and consequent coastal land loss. Mar Geol 129:189–195

STANLEY DJ, WARNE AG (1993) Nile delta: recent geological evolution and human impact. Science 260:628–634

STILLER M, ASSAF G (1973) Sedimentation and transport of particles in Lake Kinneret traced by ^{137}Cs. In: Hydrology of lakes Symposium. IAHS-AISH Publication No. 109, Helsinki, pp 393–405

STILLER M, IMBODEN DM (1986) ^{210}Pb in Lake Kinneret waters and sediments: residence time and fluxes. In: Sly PG (Ed) Sediments and water interactions. Springer, Berlin Heidelberg New York, pp 501–511

TOUSSOUN O (1922) Mémoires sur les anciennes branches du Nil à l'epoque ancienne. Mémoire de l'Institut d'Egypte 4

WATERBURY J (1979) Hydropolitics of the Nile Valley. Syracuse University Press, Syracuse